Fracture Gradient Prediction and Application[1]

B. A. Eaton
Universal Drilling and Engineering Consultants, Inc.
Houston, Texas

ABSTRACT

The subject of many technical papers in the last 20 years has been the prediction of the well-bore pressure gradients that are required to induce or extend fractures in subsurface formations. The subject merits attention because of recurring problems that arise from an inability to predict fracture pressure gradients.

Lost circulation is often a very troublesome and expensive problem when wells are drilled in both new and old oil fields. Complete loss of circulation can be disastrous. Such disasters can be avoided if techniques for calculating fracture pressure gradients had been employed in the well plans and followed accordingly. In areas of abnormally pressured formations, the prediction of fracture gradients during the well-planning stage is extremely important.

There are several methods used to determine fracture pressure gradients, however, none seem general enough to be used widely. In the paper by Hubert and Willis, overburden pressure, formation pore pressure gradient, and Poisson's ratio of rocks were independent variables that were shown to control the fracture pressure gradient.

In arriving at a new method of predicting formation fracture gradients, it was found that overburden load, Poisson's ratio, and pressure gradients vary with depth. Although the method was developed for the Gulf Coast, it should be highly reliable for all areas, provided that the variables reflect the conditions in the specific area under exploration.

INTRODUCTION

The subject of many discussions and technical papers in the last 20 years has been the prediction of the well-bore pressure gradients that are required to induce or extend fractures in subsurface formations. The subject merits this attention because of the frequently recurring problems that arise from an inability to predict fracture pressure gradients.

Encountered in several common types of operations in the oil industry are problems associated with the prediction of formation fracture pressure gradients. When wells are being drilled in both new and old fields, lost circulation is often a very troublesome and expensive problem. Complete loss of circulation has been disastrous in some cases. Many times, such disasters could have been avoided if techniques for calculating fracture pressure gradient had been employed in the well plans, and if casing strings had been set, and mud weight plans had been followed accordingly. In areas of abnormally pressured formations, the prediction of fracture gradients during the well-planning stage is extremely important. In fact, it is as important as the prediction of formation pressure gradients, which has received a great deal of attention in recent years.

Not all predictions of fracture pressure gradients are made to avoid disasters such as complete loss of circulation and blowouts. In fact, many fracture gradient predictions are made in the process of designing hydraulic fracturing stimulation of producing wells, a technique that has proven to be one of the greatest petroleum engineering accomplishments. This process was introduced in 1948 by Clark.[1] Since then, over 500,000 hydraulic fracturing jobs have been completed in the U.S. alone. The physical breakdown of subterranean formations during induced hydraulic fracturing is related to that which occurs during each of the following oilfield operations:

1. Hydraulic fracturing or fracture acidizing
2. Pressure parting in injection wells in secondary recovery operations

1. Original material for this article was published and copyrighted by Society of Petroleum Engineers, AIME

3. Lost circulation during drilling
4. The breakdown of formations during squeeze cementing
5. The breakdown of formations during plastic sand consolidation when well-bore pressures become too great.

All of these phenomena involve the creation of open fractures by applied pressure in wellbores. Such operations have provided the field data that have led to the partial understanding of formation fracturing phenomena.[2,5,6] Such data are not always consistent, especially when many geographical areas are considered. These inconsistencies have led to many arguments concerning fracture orientation and fracture gradient prediction methods.[3]

There are several published methods used to determine fracture pressure gradients. However, none of these methods appears to be general enough to be used with much reliability in all areas. In 1957, Hubbert and Willis published a classical paper that included the development of an equation used to predict the fracture extension pressure gradient in areas of incipient normal faulting.[3] Overburden stress gradient, formation pore pressure gradient, and the horizontal-to-vertical stress ratio of rocks were the independent variables that were shown to control fracture pressure gradient, the dependent variable.

In 1967, Matthews and Kelly published another fracture pressure gradient equation that is different from that of Hubbert and Willis, in that a variable "matrix stress coefficient" concept was utilized.[4] Later the same year, Costley wrote about a similar idea.[5]

Goldsmith and Wilson used a least-squares curve-fitting technique and field data from the Gulf Coast area to correlate fracture pressure gradient with formation pore pressure gradient and formation depth.[6] They noted that the fracture pressure gradient increased with increasing depth while the pore pressure gradient remained constant.

In each of these cases, the problem for which a solution was sought was to determine the bottom-hole pressure gradient required to initiate or extend a fracture. Results of the previous work show that fracture pressure gradient is a function primarily of overburden stress gradient, pore pressure gradient, and the ratio of horizontal to vertical stress. There is argument for a fourth variable in that in many cases breakdown fracture pressure gradient is greater than the fracture extension pressure gradient. However, if the fracturing fluid is able to penetrate the formation through the pores or existing cracks, there is very little difference in the two fracturing pressure gradients.

Throughout the remainder of this chapter, no distinction is made between breakdown fracture gradients and extension fracture gradients. The extension gradient will be the lower gradient of the two and is the gradient used in most design situations.

ROCK MECHANICS

Since any study of fracture gradient prediction must involve an analysis of data derived from operations that create or induce fracturing, some knowledge of underground stresses is required. Naturally occurring underground stresses resist wellbore fracturing. If effective stresses are defined as those stresses which are normal to planes in which there is no shear, the general stress condition can be defined in terms of the effectives stresses, σ_z along the vertical Z axis, and σ_x and σ_y along the horizontal X and Y axes.[3] In the absence of external forces, the stress state is caused by the sediments above the point in question, or the overburden load. Figure 1 illustrates the stress state of an element of rock buried in the earth's crust.

Overburden load, S, at a given point is supported by both the vertical bearing stress of rock particles and the fluid pressure in the pore spaces. This equilibrium of forces on an element of subterranean rock may be expressed in equation form as:

$$S = \sigma_z + p \qquad (1)$$

where:

p = pore pressure of formation fluid, psi
σ_z = vertical stress in the rock matrix grains, psi
S = overburden pressure or load, psi

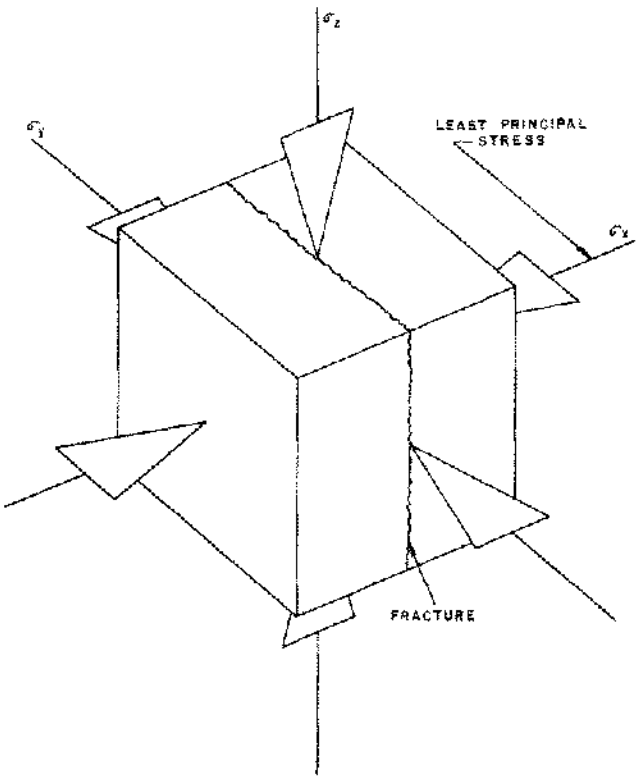

Figure 1. Stress element and preferred plane of fracture.

The physical relationship that exists in rock formations between grain stress, pore pressure, and overburden load is simulated very simply in Figure 2 for both normal pressured and abnormal pressured formations. In both cases, S equals 10,000 psi (the piston) and the counter-acting stresses are 1) the fluid pressure (pore pressure), and 2) the spring (the vertical stress in rock grains). It can easily be seen that if the fluid is not free to escape, as in case B, the pore pressure must become larger as more and more overburden load is applied. When this happens, the grain stress supports a less proportionate part of the overburden, S.

Equation 1 may be solved for the matrix stress as follows:

$$\sigma_z = S - p \tag{2}$$

In this light, σ_z, is normally known as the "net effective vertical rock stress", or "net effective overburden stress."

Under influence of vertical stress, the rock element tends to expand laterally but is prevented from doing so by the surrounding rock. This tendency creates a horizontal stress, σ_h, which under ideal conditions is equal in all horizontal directions. In this case,

$$\sigma_x = \sigma_y = \sigma_h \tag{3}$$

According to Hooke's law, the horizontal strain, ϵ_x, is expressed as:

$$\epsilon_x = \frac{\sigma_x}{E} - \nu\frac{\sigma_y}{E} - \nu\frac{\sigma_z}{E} \tag{4}$$

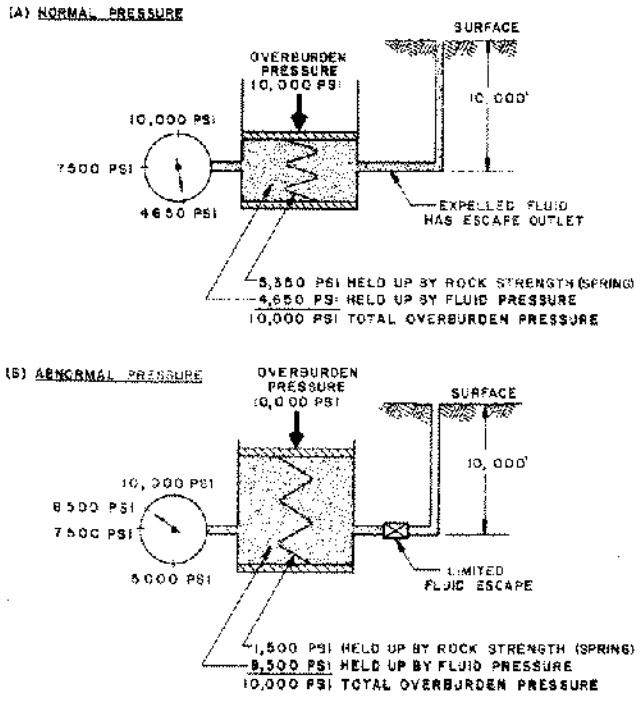

Figure 2. Earth stress model.

where:

ϵ_x = strain in the horizontal x direction

$= \epsilon_y = \epsilon_h$

E = Young's modulus

ν = Poisson's ratio

In the elastic zones of the earth's crust, since no horizontal motion can occur due to surrounding rock, ϵ_x is essentially zero. Therefore, when
$e_x = 0$ in Equation 4 and $\sigma_x = \sigma_y = \sigma_h$

$$0 = \frac{\sigma_h}{E} - \nu\frac{\sigma_h}{E} - \nu\frac{\sigma_z}{E} \tag{5}$$

or

$$\sigma_h = \left(\frac{\nu}{1-\nu}\right)\sigma_z \tag{6}$$

If the expression for σ_z from equation 2 is substituted into equation 6, the following is obtained:

$$\sigma_h = \left(\frac{\nu}{1-\nu}\right)(S-p) \tag{7}$$

If one examines equation 6, it becomes obvious that σ_z is always greater than, or at least equal to σ_h, where tectonic forces are negligible. Only when $\nu = 0.50$ does $\sigma_h = \sigma_z$. Poisson's ratio, ν, for rocks has been measured and usually ranges between 0.20 and 0.35.[7] However, ν becomes equal to 0.5 for incompressible materials in the plastic failure stress state. Therefore, it is quite possible for values of Poisson's ratio for rocks buried at 20,000' to be much greater than measured values in the laboratory for the same rocks.

Example problem

A rock element is buried at a depth of 11,000'. The overburden load is 10,000 psi, while the pore pressure in the element is 5,200 psi. Poisson's ratio for this rock in this stress state is 0.25. Determine:

1. σ_z, the effective overburden stress in the element.
2. σ_h, the effective horizontal stress in the element.

Solution:

1. Using equation 2

$$\sigma_z = 10{,}000 - 5{,}200$$
$$= 4{,}800 \text{ psi}$$

2. Using equation 6

$$\sigma_h = \frac{(0.25)}{(1-0.25)} \cdot 4{,}800$$
$$= 1/3 \cdot 4{,}800$$
$$= 1{,}600 \text{ psi}$$

The preceding brief section on simple rock mechanics illustrates the variables that relate the vertical and horizontal stresses in a rock element buried in the elastic zones

of the earth's crust. These are important in fracture gradient prediction work.

FRACTURE PRESSURE GRADIENT PREDICTION

In order for a fracture to be extended in a rock formation from a wellbore, the pressure in the wellbore must be great enough to first overcome the least principle stress, whether that be σ_z, σ_x, or σ_y. The wellbore pressure must also be greater than the formation pressure to cause fluid to flow back in the fracture. Hubbert and Willis analyzed this behavior in classic fashion. Their equation describing fracture extension pressure is:

$$p_w = \sigma_h + p \tag{8}$$

They further assumed that $\sigma_h = 1/3\sigma_z$ (equivalent to $\nu = 0.25$) and in this manner equation 8 becomes

$$p_w = 1/3\sigma_z + p$$

$$= 1/3\ (S-p) + p$$

$$p_w = 1/3\ (S + 2p) \tag{9}$$

After dividing both sides of equation 9 by the vertical depth, D, of the formation, the "pressure gradient" form is produced.

$$\frac{p_w}{D} = 1/3\left(\frac{S}{D} + \frac{2p}{D}\right) \tag{10}$$

Equation 10 is what is known as the Hubbert and Willis equation for fracture pressure gradient prediction. Hubbert and Willis assumed that the overburden stress gradient S/D, was constant and equal to 1.0 psi/ft. Under these conditions, the fracture gradient is calculated to be a constant with increasing depth for all normally pressured formations. Using this latter assumption, equation 3.10 becomes:

$$\frac{p_w}{D} = 1/3\ (1.0 + \frac{2p}{D}) \tag{11}$$

Example problem 3.2

(a) Calculate the fracture pressure gradient of a formation at 10,000' whose formation pore pressure gradient is 0.465 psi/ft. (4,650 psi at a depth of 10,000'). (b) Calculate the fracture gradient at 5,000' when the pore pressure gradient is 0.465 psi/ft. In both cases, use equation (11) (c) What is the fracture pressure in each case?

Solution:

In both cases (a) and (b), equation 3.11 gives the same result. When dealing with pressure gradients, not pressures, equation 3.11 is independent of depth.

(a) $\frac{p_w}{D} = 1/3\ [1.0 + 2\ (0.465)]$

$= 0.65$ psi/ft at 10,000'

(b) $\frac{p_w}{D} = 1/3\ [1.0 + 2\ (0.465)]$

$= 0.65$ psi/ft. at 5,000'

(c) for case (a)

$\frac{p_w}{10{,}000} = 0.65$ $p_w = 6{,}500$ psi

for case (b)

$\frac{p_w}{5{,}000} = 0.65$ $p_w = 3{,}250$ psi

It can easily be seen from the preceding example that the simplified Hubbert and Willis method of fracture gradient prediction results in values that are equivalent for any well depth provided the pore pressure gradients are the same. This is known to be untrue for many cases in the Gulf Coast. Actually, Equation 11 predicts values that are usually too low, compared with values from field data.

Several authors have questioned the foregoing assumptions.[4,5,9] Hence, it seems worthwhile to review and compare the various techniques used to calculate fracture pressure gradients. To do so, the pressure data given in Figure 3 and 4 were used to calculate the fracture pressure gradient by several methods.

Equation 11 was used for comparative purposes to calculate Curve 2 of Figure 4, using the pressure gradient curve data (Curve 1 of Fig. 5) as determined from the log data of Figures 3 and 4. Note that p_w/D increases only when p/D increases. Similarly, the log data for Well B were used with Figure 4 to determine the pressure gradient of Well B. The results make up Curve 1 of Figure 6. Curve 2 of Figure 6 shows the fracture gradient computed by the Hubbert and Willis equation. The same behavior is to be observed as in the first example. However, experience has shown that p_w/D increases with depth, regardless of the pressure behavior, until the abnormal pressure section is traversed. Then p_w/D may decrease as shown by the other curves in Figures 5 and 6.

Matthews and Kelly presented a fracture gradient equation similar to Equation 11. However, they introduced the concept of a variable horizontal-to-vertical stress ratio. Figure 7 is a reproduction of their curves showing the variable stress ratio as a function of depth for two areas. Again one must assume that the overburden load is 1.0 psi/ft. To calculate a fracture gradient by this method one must use the following procedure.

1. Obtain the formation pore pressure.
2. Determine the effective stress, $= 1.0D - p$.
3. Determine the depth D_i for which the matrix stress would be the normal value:

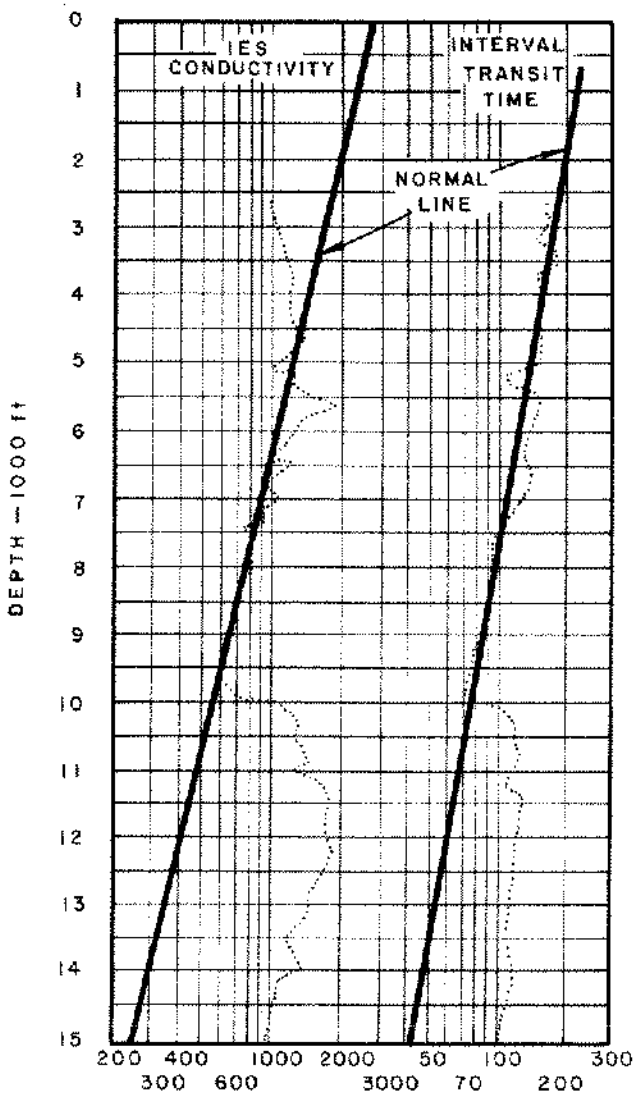

Figure 3. Log data from Frio Formation, Nueces County, Texas.

$$D_i = \frac{\sigma}{0.535}$$

4. Use the value of D_i from the preceding step with Figure 7 to determine K_i.

5. With the resulting data, calculate the fracture gradient using the Matthews and Kelly fracture gradient equation, which follows:

$$\frac{p_w}{D} = K_i \left(\frac{\sigma}{D}\right) + \frac{p}{D} \qquad (12)$$

(Note: Matthews and Kelly call this the breakdown gradient and say that it is higher than the fracture extension gradient.)

6. Plot the fracture gradient as a function of depth.

In this manner, Curve 4 of Figure 5 and Curve 3 of Figure 6 were generated. The effect of depth and formation pressure is readily evident. However, there appear to be two weaknesses in the approach, one of which is the assumption that the overburden stress is equal to 1.0 psi/ft of depth. The other weakness is that the stress ratio, K_i, used in calculating the fracture gradient in abnormally pressured formations is that of the deepest normally pressured formation. The Matthews and Kelly approach represents a significant advancement in fracture gradient technology, and the variable stress ratio concept is quite valid when compared with field data analysis.

Recently, Goldsmith and Wilson found that the presently existing techniques for calculating fracture gradients were inadequate. Using a great deal of data on lost circulation and squeeze pressure, they developed empirical equations, using least-squares curve-fitting, that appear to predict very well the fracture gradients for a localized area. The equations are long and somewhat difficult to use, but this technique was employed in calculating Curve 5 of Figure 5. The vast disagreement of these techniques is well illustrated.

Costley recently published yet another technique that is similar to the Matthews and Kelly method. The same basic assumptions are involved, therefore, the method will not be discussed further. Nevertheless, the data published by Costley were used with other data to develop the Eaton[9] method that follows.

Throughout the remainder of this chapter it is postulated that the assumptions leading to equations 6, 7, and 8 are valid. If the value of σ_h from equation 7 is then inserted into equation 8, the result is:

$$p_w = \left(\frac{\nu}{1-\nu}\right)(S-p) + p \qquad (13)$$

and by dividing through by formation depth, D, we obtain:

$$\frac{p_w}{d} = \left(\frac{\nu}{1-\nu}\right)\left(\frac{s-p}{D}\right) + \left(\frac{P}{D}\right) \qquad (14)$$

Equation 14 is known as "Eaton's Fracture Gradient Equation". Note that the units are in psi/ft. for all terms. It can be seen that fracture pressure gradient is a function of Poisson's ratio, formation pore pressure, and overburden load pressure. The problem then boils down to determining the function of each variable with formation depth.

Since it is accepted here that abnormal formation pressure gradients may be determined from logs[8], that aspect of the problem is solved. The next steps are to assume that the overburden stress gradient is 1.0 psi/ft., then to solve Equation 14 for the stress ratio group:

$$\left(\frac{\nu}{1-\nu}\right) = \frac{\frac{p_w}{D} - \frac{p}{D}}{\frac{S}{D} - \frac{p}{D}} \qquad (15)$$

and to evaluate Equation 15 with field data.

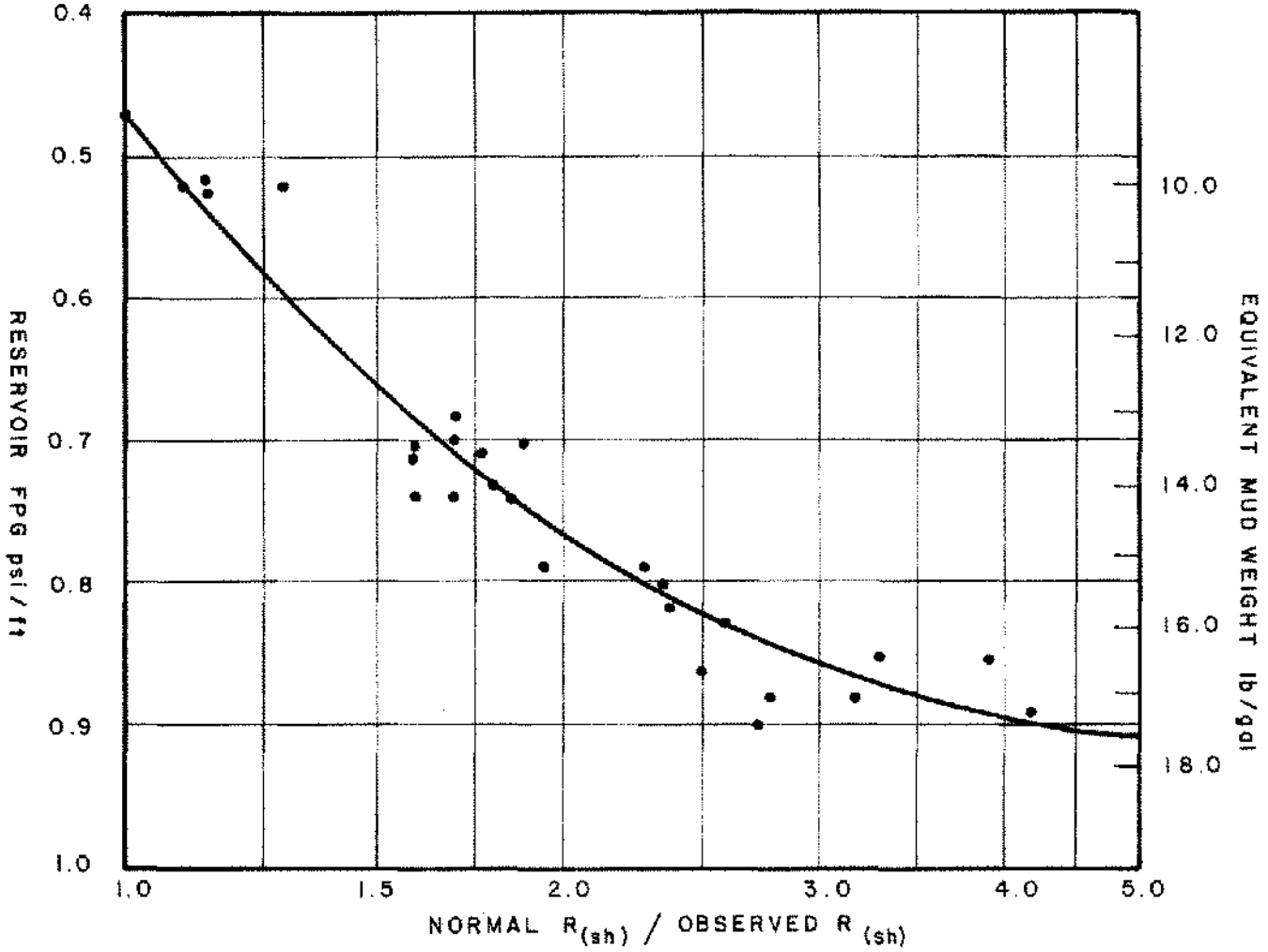

Figure 4. Relationship between shale resistivity parameter $R_{n(sh)}/Rob(sh)$ and reservoir fluid pressure gradient.

A great deal of data from the analysis of hydraulic fracturing treatments in West Texas was published by Crittendon[9]. These data were used to develop the left curve of Figure 8. It can be seen that for the producing formations of the West Texas area, the assumptions S/D = 1.0 and $\nu = 0.25$ are valid.

Data given by Costley were used to back-calculate the middle Poisson ratio curve of Figure 8. Note the curvature of the trend of Poisson ratio vs. depth for the Gulf Coast area. This is caused by the sediments being younger and more compressible near the surface, but less compressible and more plastic with depth. For this reason, the curve approaches 0.5 as an upper limit. This limit is the Poisson ratio of an incompressible material in the plastic failure environment.

Example results of fracture pressure gradient calculations using the middle Poisson ratio curve of Figure 8 and Equation 14 are included for comparative purposes. These are shown by Curve 6 of Figure 5 and Curve 4 of Figure 6.

From the preceding calculations, it becomes evident that the variation of overburden stress with well depth must be determined where formations are compressible, such as in the Gulf Coast area. A composite group of density logs from many Gulf Coast wells are available. These logs were used to plot bulk density vs. depth, which is shown in Figure 9. The values for bulk density were read at the mid-point of each 1,000-ft. interval and averaged step by step downward to 20,000 ft, of depth. In this manner, the overburden stress curve of Figure 10 was produced. The value of overburden stress read from the curve at any depth represents the real average overburden gradient at that specific depth. Further averaging need not be done.

The same procedure was used for similar data from wells in the Santa Barbara Channel. Bulk densities from logs and the resulting overburden stress gradient curve are shown in Figures 11 and 12, respectively, with the results being similar to those given in Figures 9 and 10. It was concluded that variable overburden stress gradient curves,

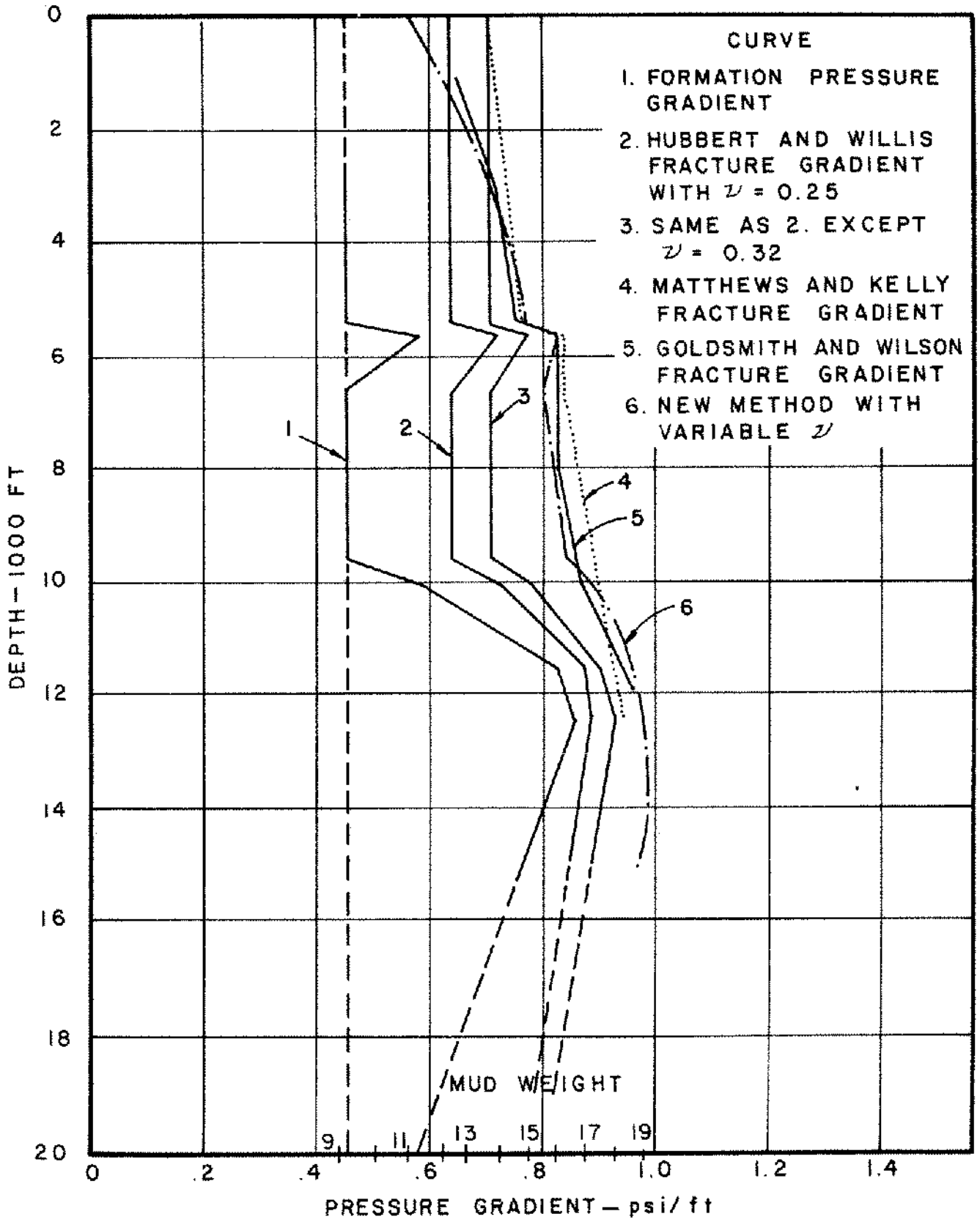

Figure 5. Formation and fracture pressure gradients.

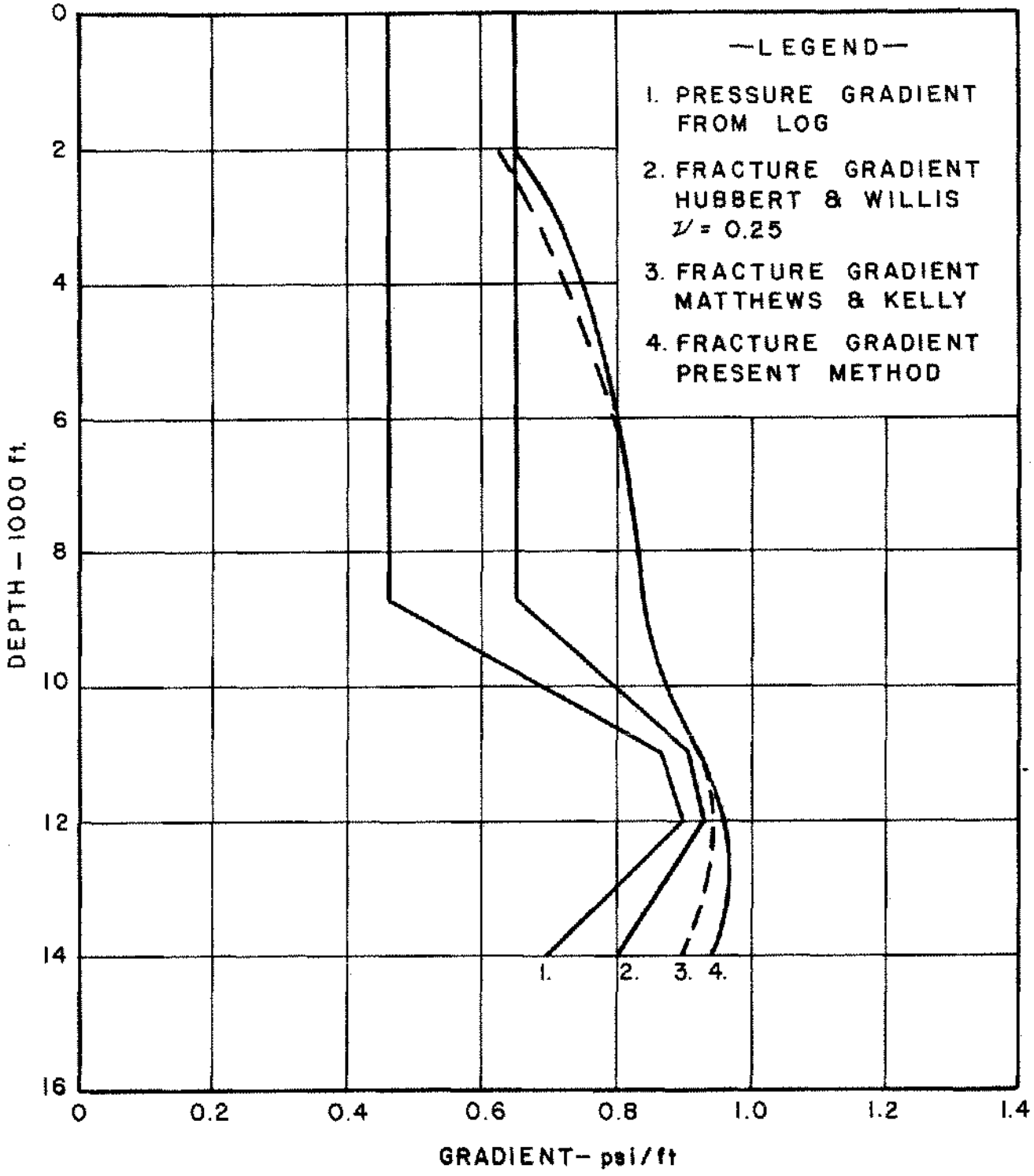

Figure 6. Well B, East Cameron Field. Fracture pressure gradient comparison.

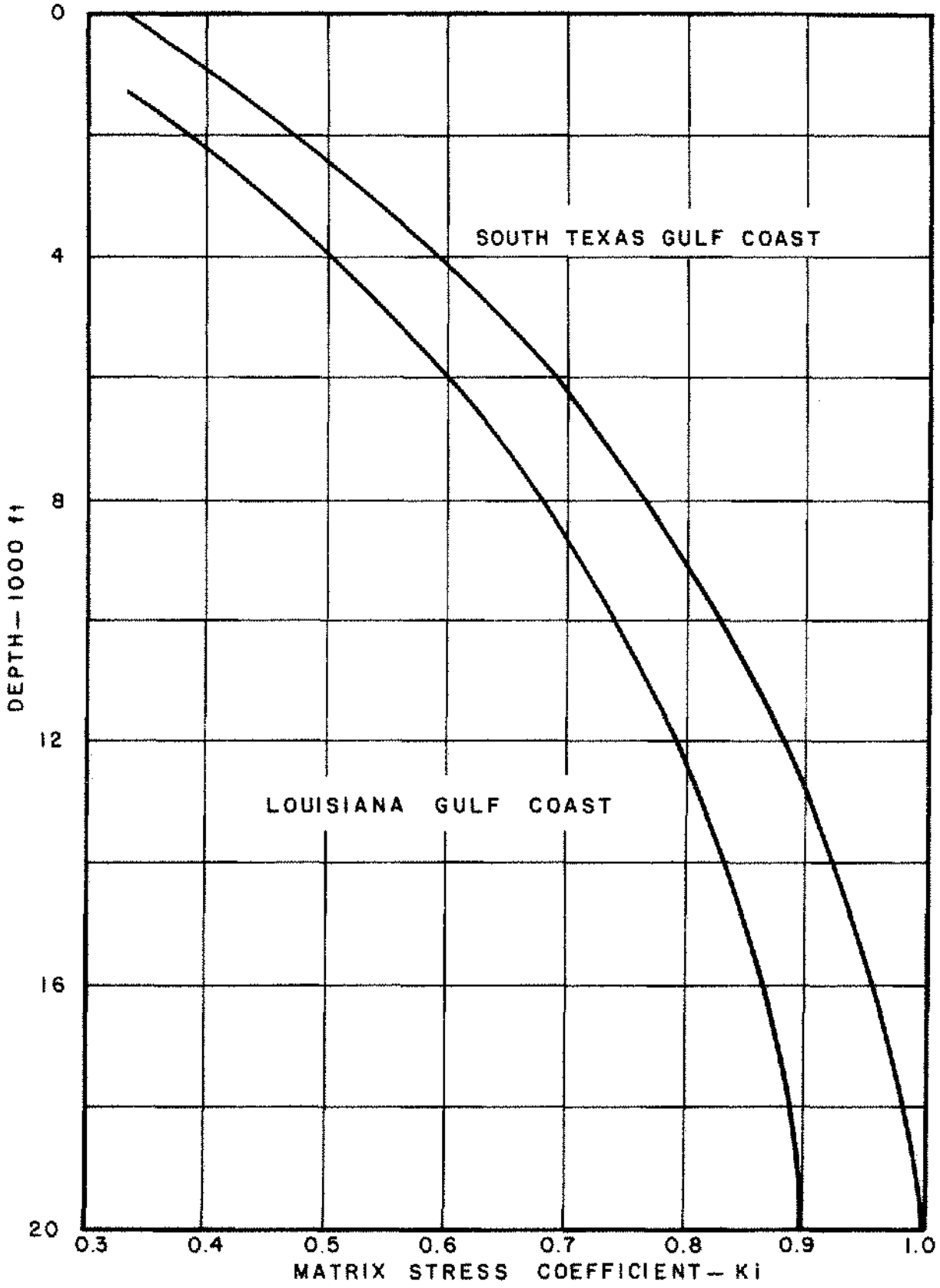

Figure 7. Matrix stress coefficient.

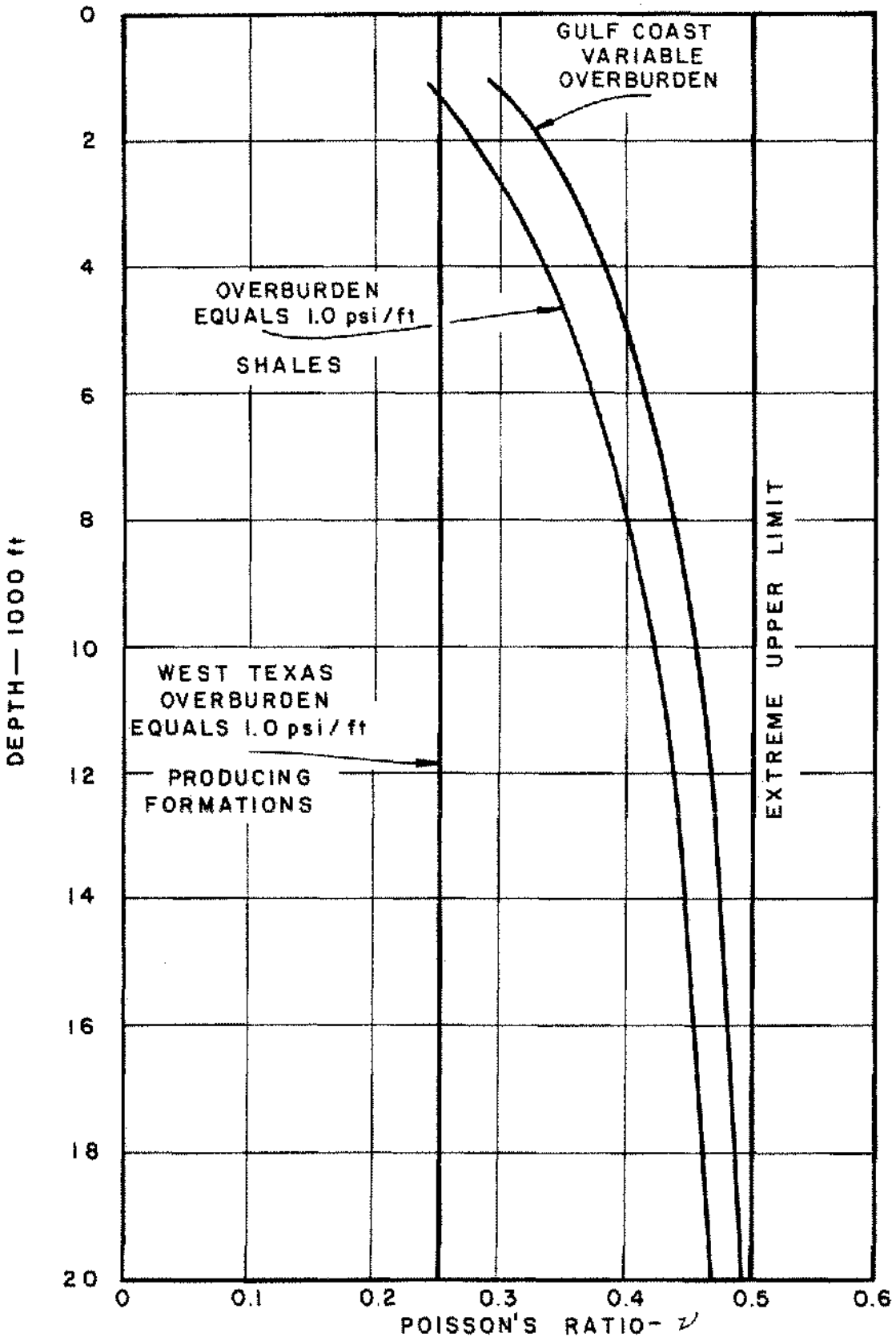

Figure 8. Variations of Poisson's ratio with depth.

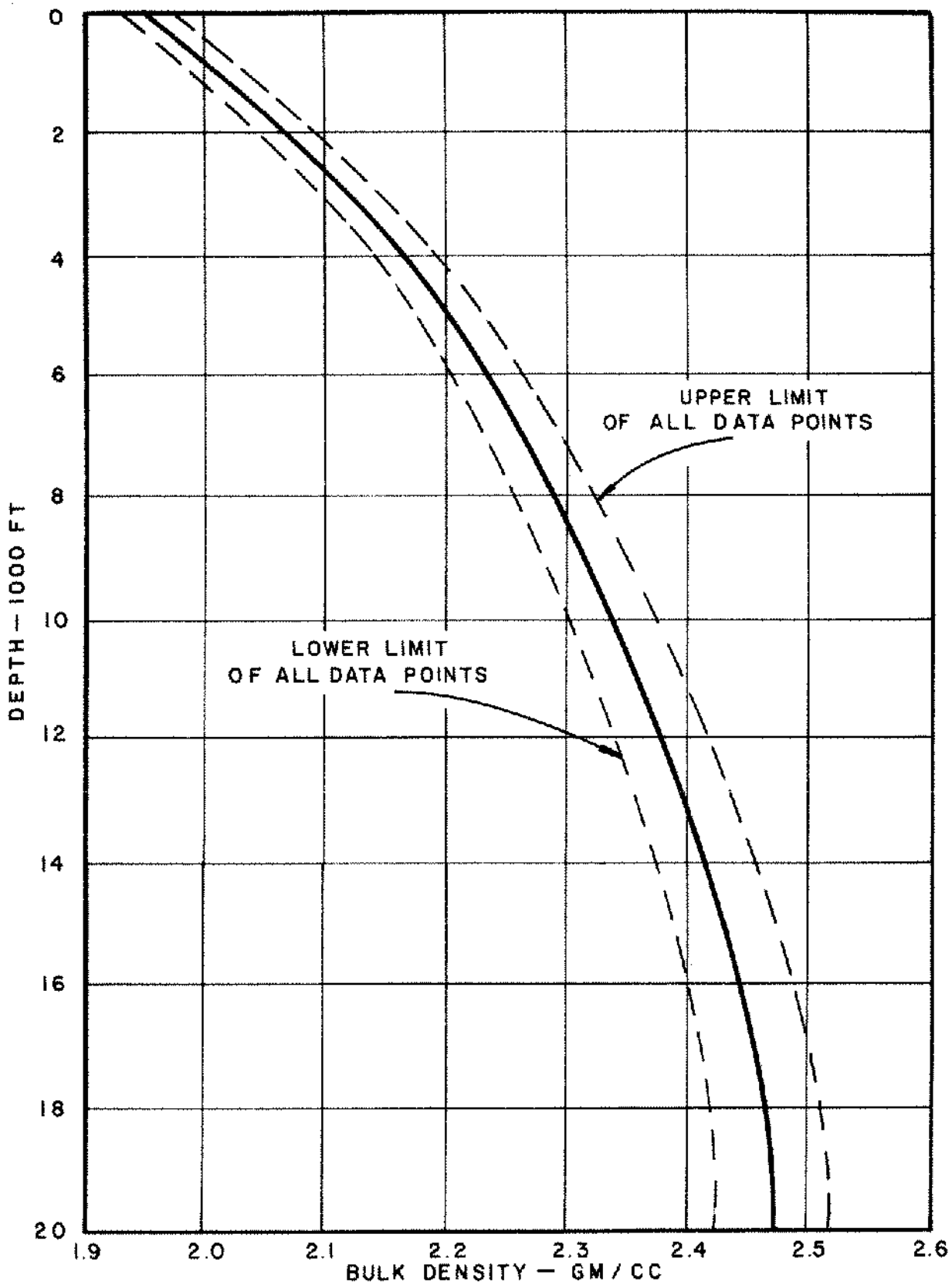

Figure 9. Composite bulk density curve from density log data for the Gulf Coast.

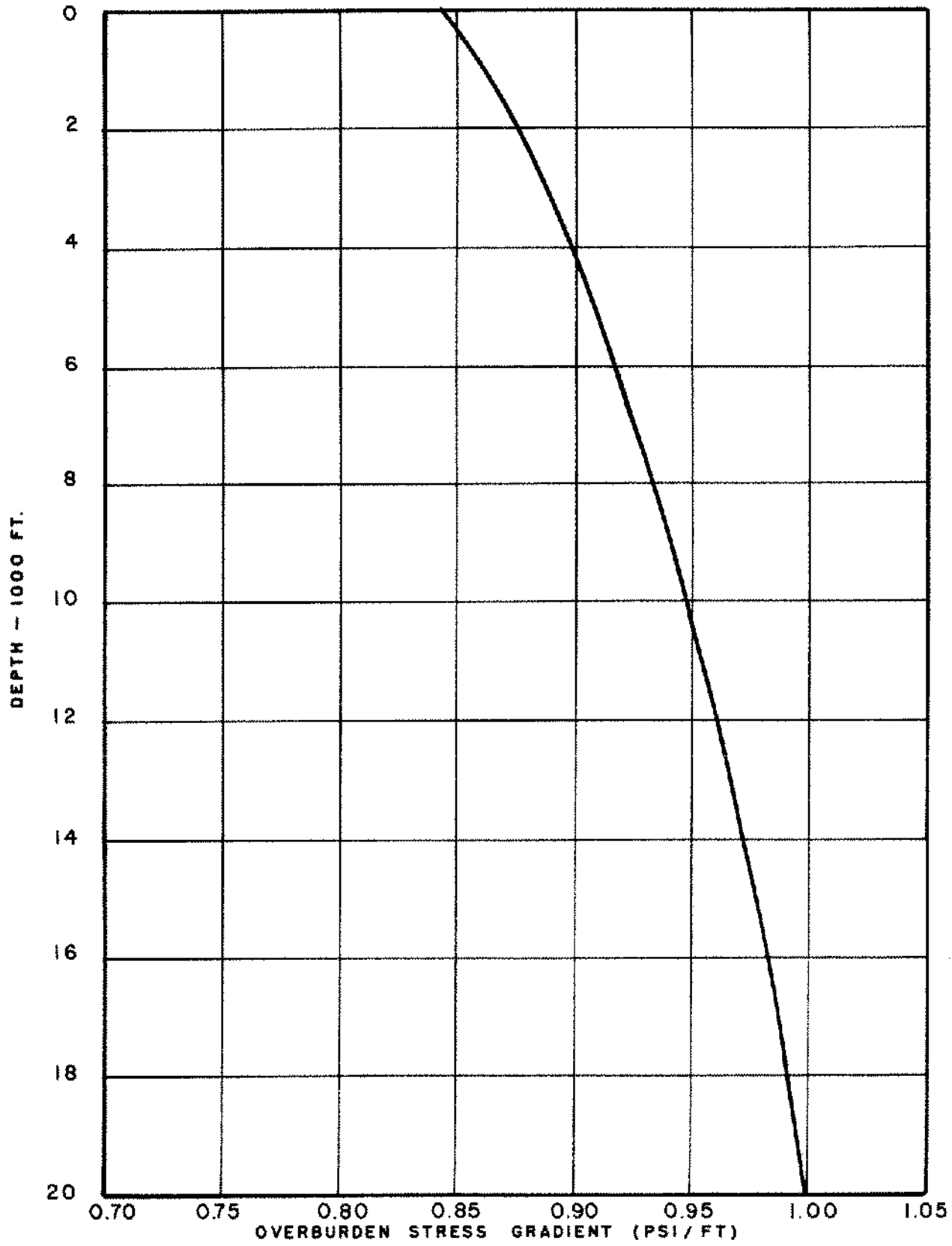

Figure 10. Composite overburden stress gradient for all normally compacted Gulf Coast formations.

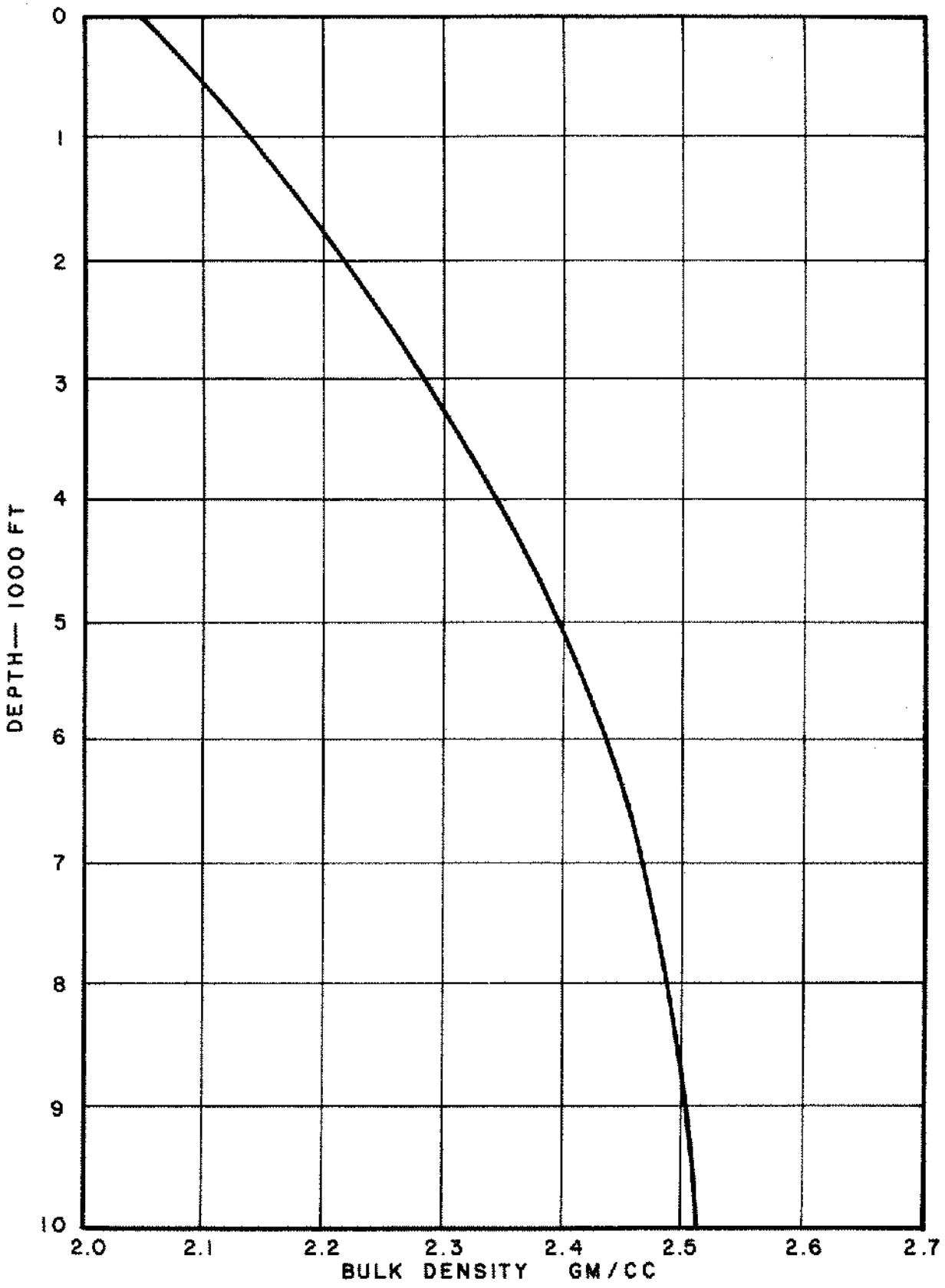

Figure 11. Bulk density curve from density logs, Santa Barbara Channel.

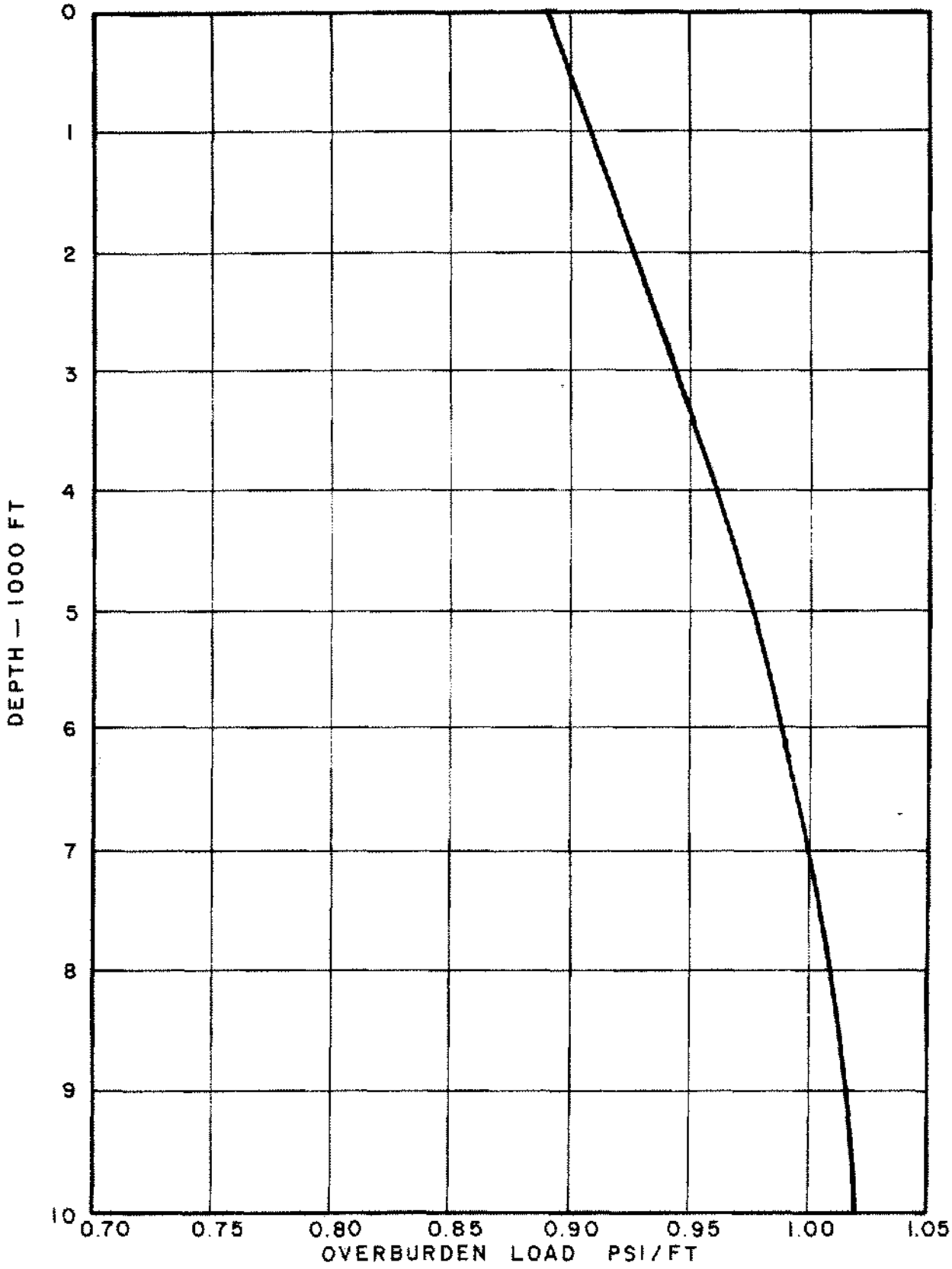

Figure 12. Overburden stress gradient, Santa Barbara Channel.

as determined from density logs of good quality, are far superior to any assumed constant number.

Based on Equation 15, the same field data, and Figure 10, the Poisson ratio trend for the Gulf Coast area was back-calculated and plotted on the right side of Figure 8. Note that this curve approaches the middle curve at greater depths where the overburden stress gradient does approach 1.0 psi/ft. It was concluded that Figures 8 and 10 could be used with formation pressure data and Equation 14 to predict accurately the fracture gradients in the Gulf Coast. The same method will apply in other areas, provided that the overburden stress gradient and Poisson ratio curves are determined from good data.

Figures 8 and 10 and equation 14 were combined to calculate the lines on Figure 13 for the Gulf Coast area. Such an easy to use chart could be developed for any area. A nomograph for solving equation 14 is given in Figure 14.

Example problem 3

Calculate the fracture pressure gradient of a formation at 3,000' in the Gulf Coast where the pore pressure gradient is 0.50 psi/ft. (a) Use equation 14; (b) use Figure 13; (c) use Figure 14; (d) what is the equivalent mud weight?

Solution:

(a) First determine the overburden gradient from Figure 10 and Poissons's ratio from Figure 8

$$S/D = 0.88,\ \nu = 0.37$$

then,

$$\frac{p_w}{D} = \left(\frac{0.37}{1-0.37}\right) \cdot (0.88-0.50) + 0.50$$

$$= 0.723 \text{ psi/ft.}$$

From Figure 13

(b) $\frac{p_w}{D} = 0.72$ psi/ft

(c) $S/D = 0.88, = 0.37$

$\frac{p_w}{D} = 0.72$ psi/ft (From Figure 14)

(d) equivalent to the head of 3,000' of 13.9 ppg mud

To demonstrate better how to apply this method of predicting fracture gradients, an example follows, showing how the technique should be employed in drilling well plans.

1. Figure 15 shows a plot of resistivities for a well in the East Cameron area. Data from Figure 15 are used with Figure 4 to produce the formation pressure curve of Figure 16. Mud weights for this area should be determined in this manner during the well planning stage. The mud weight scale at the bottom of Figure 16 and the formation pressure gradient curve dictate the minimum mud weight program.

2. The next step is to determine and plot fracture gradient vs. depth. (This is illustrated in Figure 16, which shows five fracture gradient curves.) It is assumed that the overburden gradient averages 0.8 psi/ft all the way down. The graphic solution of Equation 14 shown by Figure 14 is used with the variable Poisson's ratio curve (right-hand curve of Figure 8) to find the fracture gradient vs. depth. The process is repeated for assumed overburden stress gradients of 0.9, 1.0, and 1.1 psi/ft. These four fracture gradient curves are not correct, because the overburden gradient varies with depth according to the curve of Figure 10. However, all that must be done to arrive at the correct fracture gradient curve is to use Figure 10 and interpolate between the various gradients of Figure 16. The interpolation is shown as the correct fracture gradient curve on Figure 16. Note that near surface, the curve is between the 0.8 and 0.9 curves, and at the 4,000 ft. mark it crosses the 0.9 curve and approaches the 1.0 curve with depth. This illustrates somewhat elaborately the effect of overburden stress gradient on fracture pressure gradient. However, in actual practice, only the true fracture gradient should be used.

3. The casing points can be selected by making use of the formation pressure gradient curve (minimum mud weight curve) and the true fracture gradient curve. In the example of Figure 16, surface pipe was set at 3,100 ft. If we assume that minimum mud weights were used during drilling, a protective string of pipe must be set at no deeper than 10,400 ft. A vertical line from the pressure gradient curve at 10,400 ft. extends upward to a point slightly above that representing the surface pipe shoe. In this case, breakdown and lost circulation would not occur. However, if drilling were to continue to 11,000 ft. before a protective string is set, breakdown would occur. A vertical line from the pressure gradient curve at the 11,000 ft. mark extends up and intersects the fracture gradient curve at the 5,000 ft. mark. Breakdown would occur anywhere between
5,000 and 3,100 ft. of depth. This is simply to say that casing points should be selected by using both the formation pressure and the fracture gradient plots. All of the foregoing serves to illustrate the application of fracture gradient prediction techniques in drilling well plans.

OTHER APPLICATIONS

A knowledge of fracture gradient prediction methods is extremely useful in such everyday operations as cementing, sand consolidating, matrix and fracture acidizing, and hydraulic fracturing.

Another important application is in secondary recov-

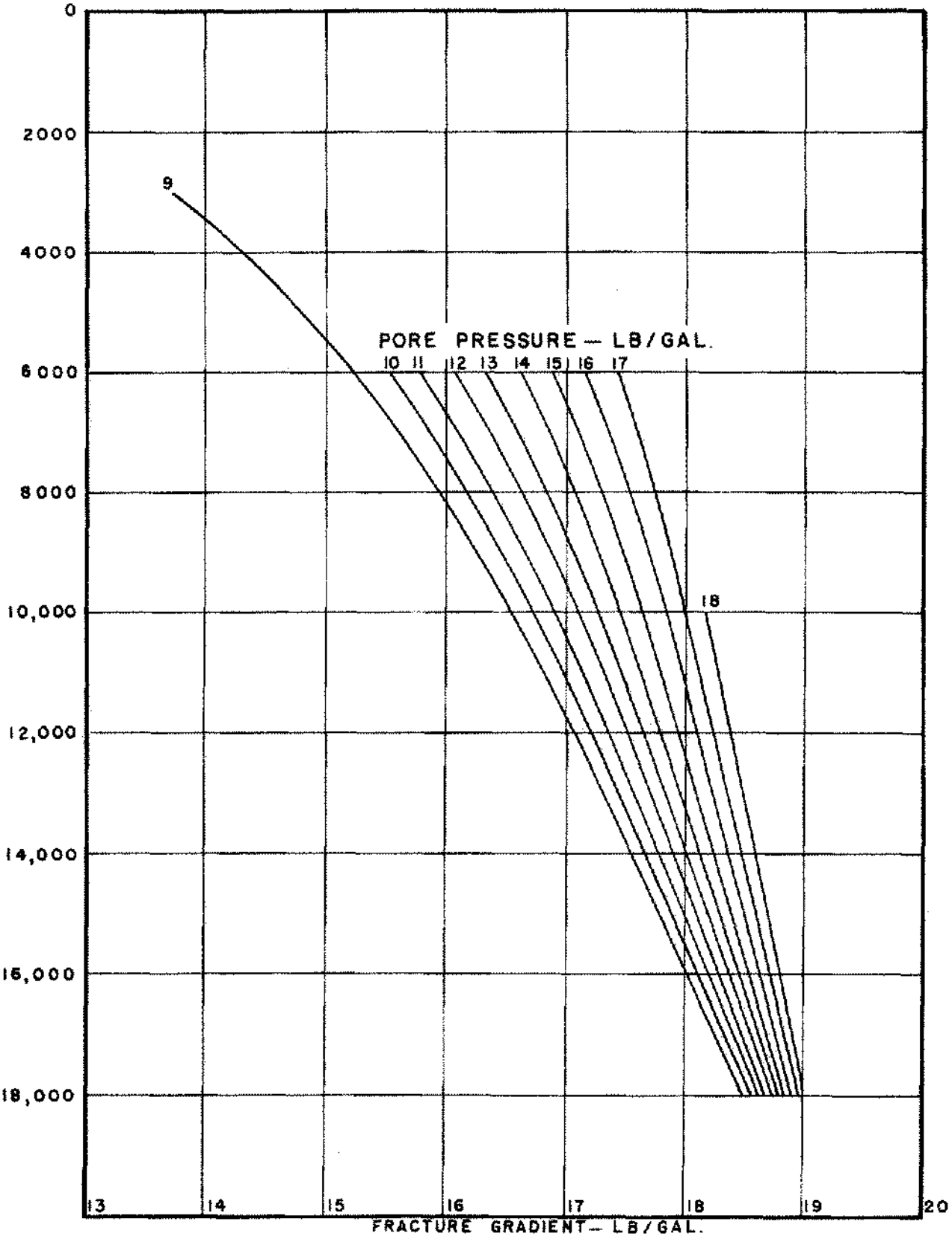

Figure 13. Gulf Coast fracture gradient curves.

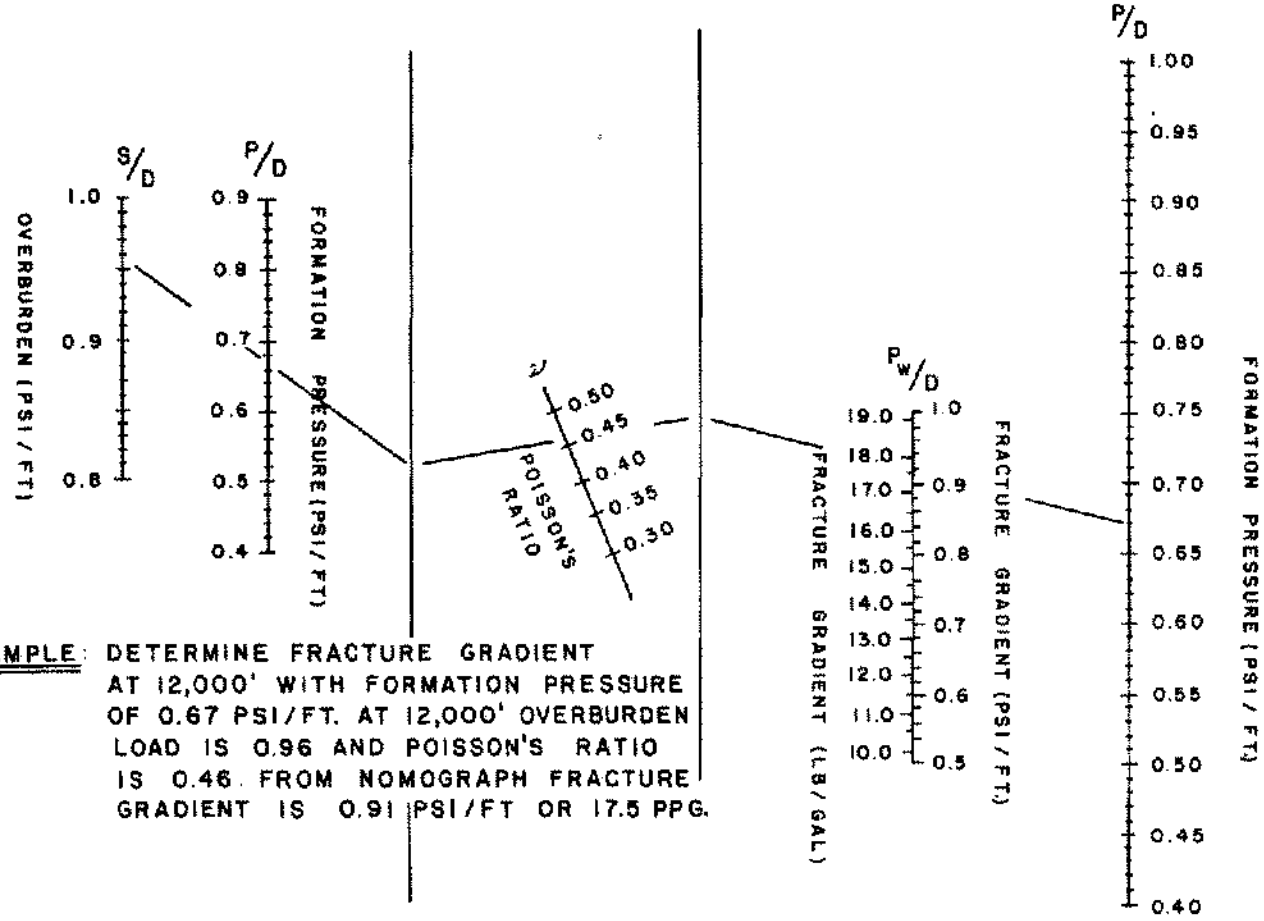

Figure 14. Fracture gradient nomograph.

ery. In most injection operations, it is desirable to stay below the fracturing pressures to prevent channeling from injector to producer. Of course, in the event that such vertical fractures all line up parallel with lines of injectors, good linear sweep patterns result. In such cases, the general direction of the fractures should be determined and injection and producing wells should be lined up to take advantage of induced fractures.

In many cases, injection is started in old wells that have been producers for years. Here the formation pressures are usually very low in the surrounding formation. Low formation pressures cause low fracture pressures, much the same as high formation pressures cause high fracture pressures. Equation 14 predicts this behavior. However, more vivid proof is given in Figure 17, in which the results of a pressure-rate test are shown. Fracturing occurred when a gradient of 0.57 psi/ft. was reached, as shown by the sudden change in slope at about 700 B/D injection. New in-fill wells in the same area are hydraulically fractured with gradients of 0.68 to 0.70 psi/ft. The relatively low fracture gradients of old producers are due to low formation pressures. Many old producing wells are fractured unintentionally when converted to injection wells. The pressure in the producing formation is so low that it cannot withstand even the gradient of fresh water.

One more example of the effect of formation pressure on fracture gradient is that three pressure-rate tests were run on a California injector on December 13, 1961; June 11, 1962; and December 3, 1962. Fracture pressure gradients were determined at sudden changes in slope of pressure-rate plots. These gradients were 0.748, 0.864, and 0.993 psi/ft. on their respective dates. These data illustrate how the fracture pressure gradient is affected by changes in formation pressure around a wellbore.

Filsenthal and Ferrell illustrated the pore pressure effect on the fracturing gradients in low permeability reservoirs.[10] They also showed that a back-calculated value of Poisson's ratio equal to 0.30 most usually fits these types of rocks. Their data are shown in Figures 18–21, and these data agree with the experience of this author.

Example problem 4

What is the expected value of Poisson's ratio of a formation that fractured under the following conditions:

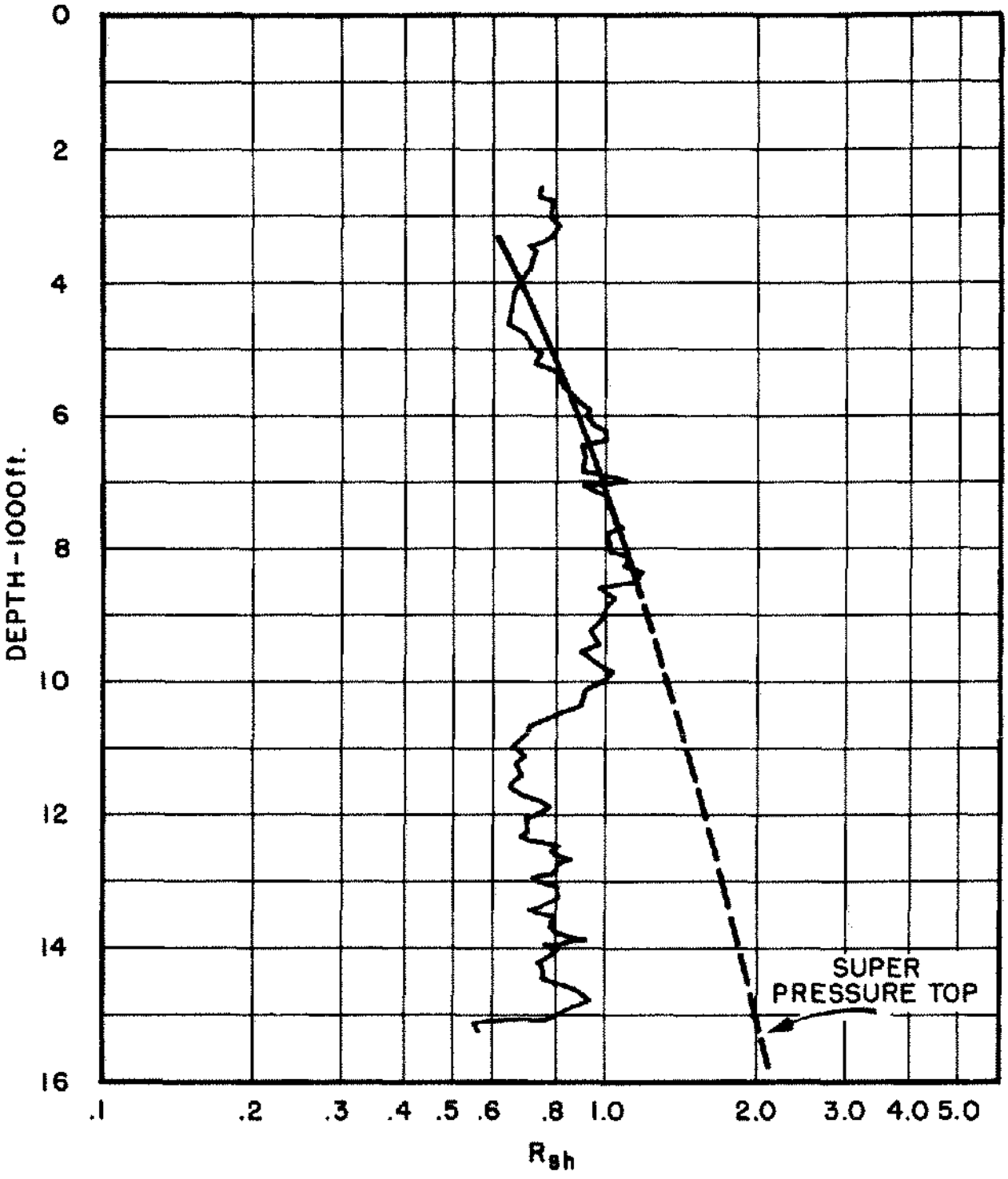

Figure 15. Log data, Welf C, East Cameron area.

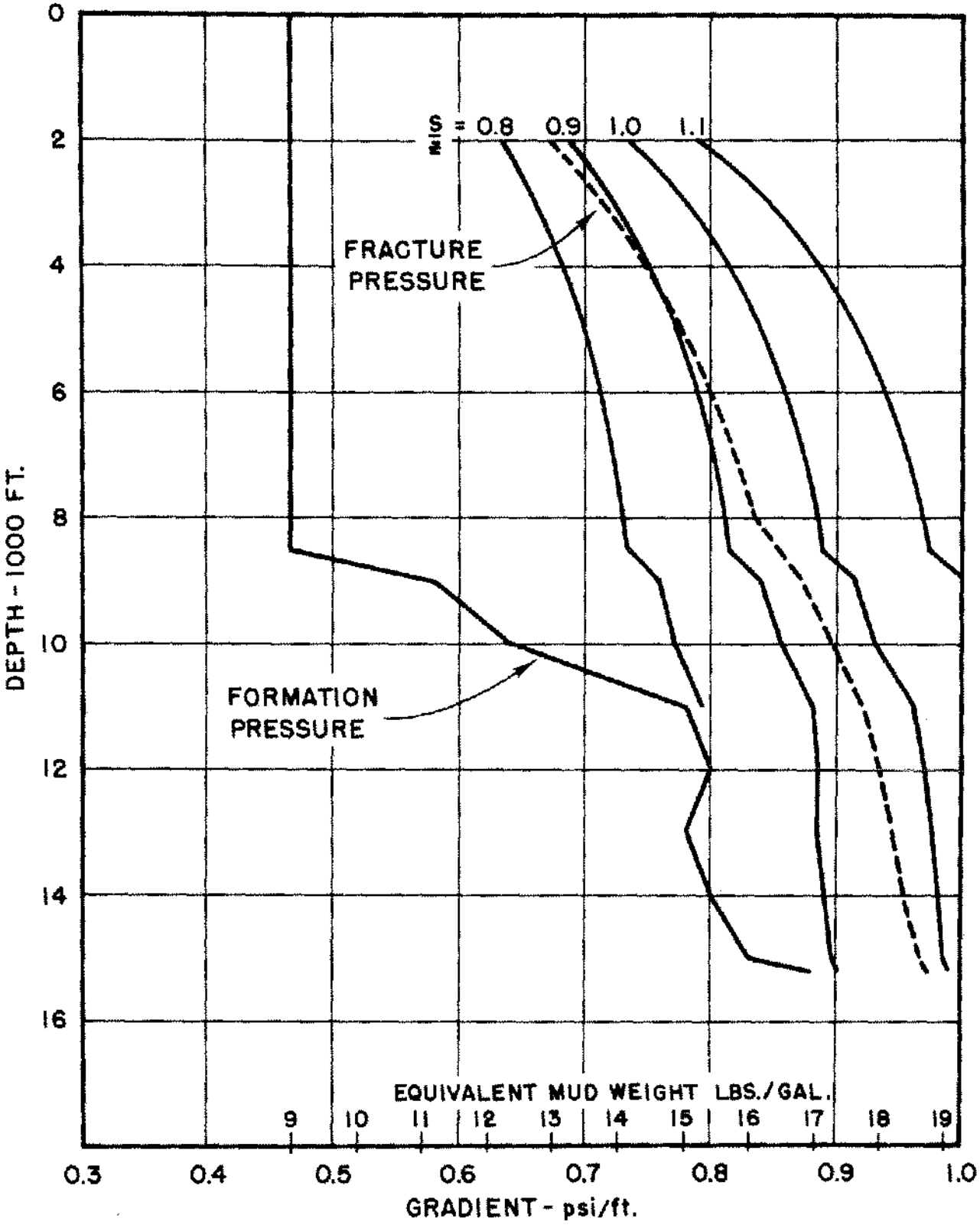

Figure 16. Fracture gradient with variable overburden and Poisson ratio included, Well C, East Cameron area.

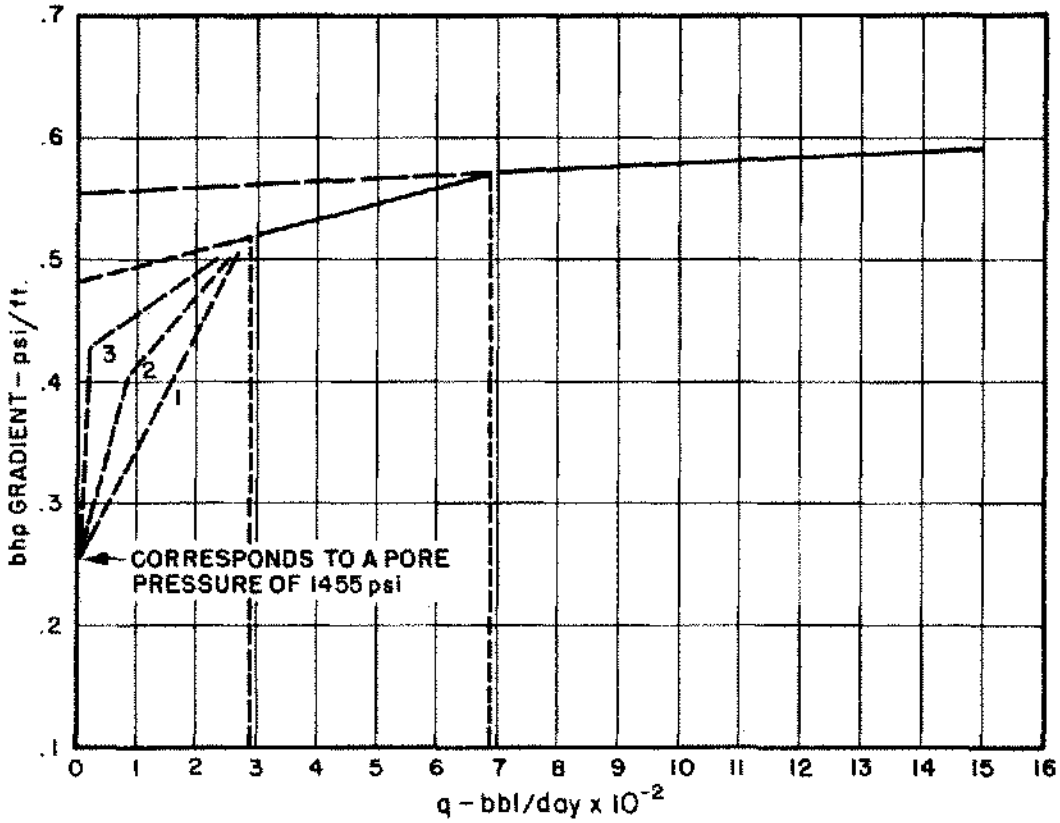

Figure 17. Fracture gradient of a West Texas water injection well.

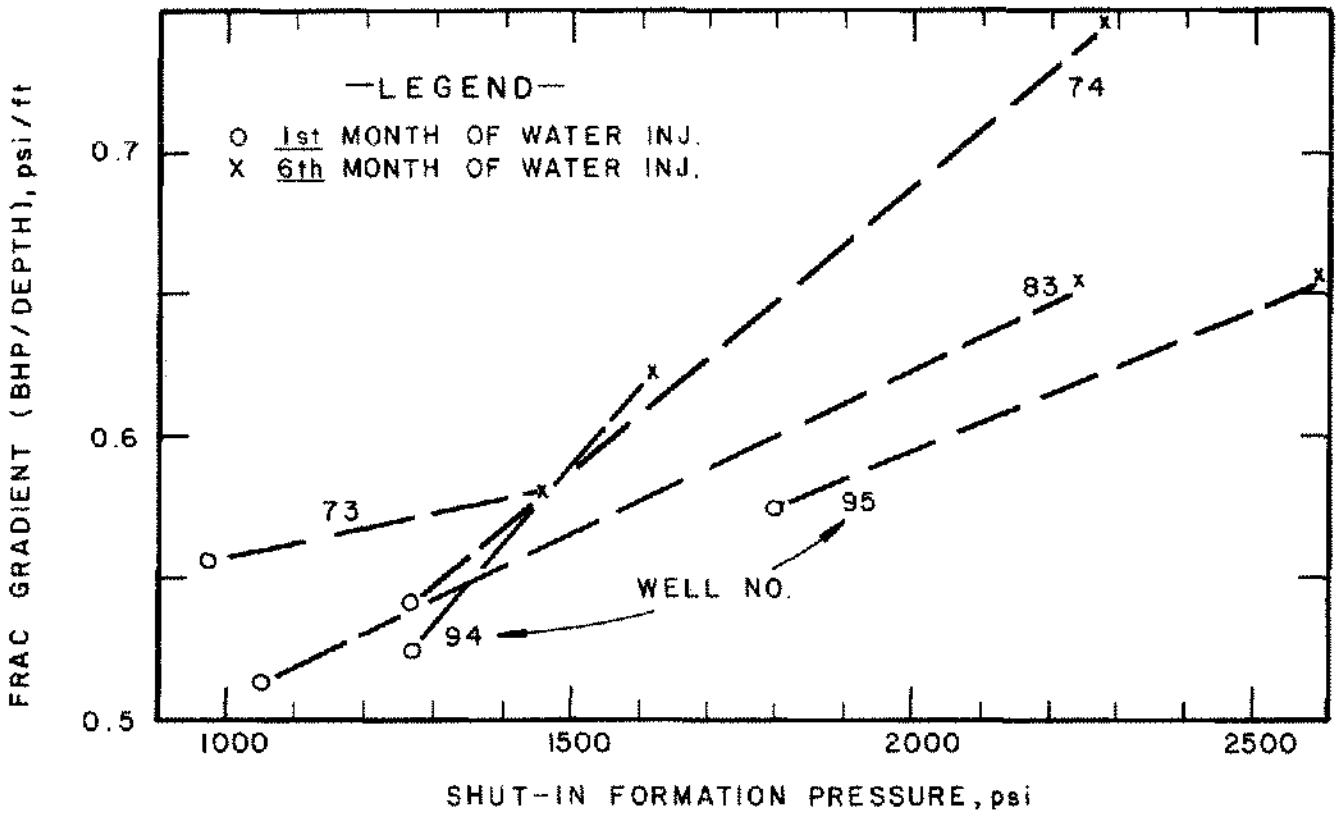

Figure 18. Increase in fracturing gradients with increase in shut-in formation pressures.

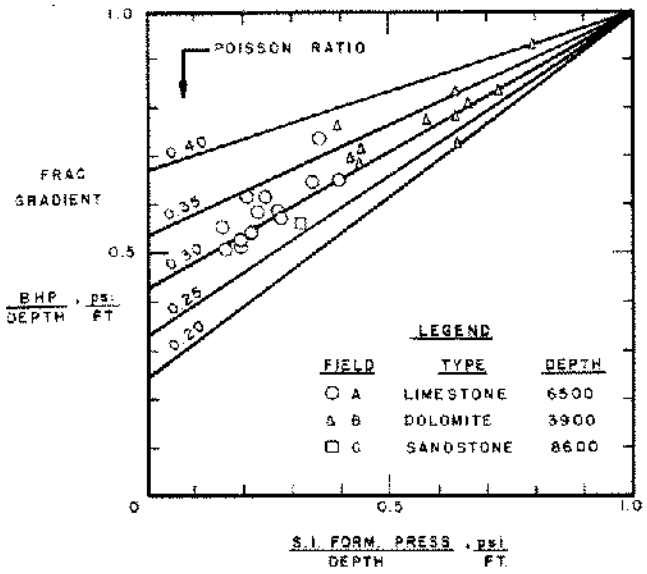

Figure 19. Field-observed fracturing gradients vs. shut-in formation pressure: depth ratios for three low-permeability reservoirs. Poisson ratio curves were derived from formation fracturing theory.

1. Pore pressure measured and found equal to 1,455 psi
2. Formation Depth–5,700 feet
3. Fracturing pressure gradient as determined from a pressure rate test was 0.57 psi/ft.
4. Formation type-carbonate

Solution:

Using equation 15

$$\frac{\nu}{1-\nu} = \frac{0.57 - \frac{1455}{5700}}{\frac{5700 - 1455}{5700}}$$

$$\frac{\nu}{1-\nu} = 0.333$$

$$\nu = 0.25$$

DEVELOPING THE TECHNIQUE FOR OTHER AREAS

The data necessary to develop this method for other tectonically relaxed areas of the earth are as follows:

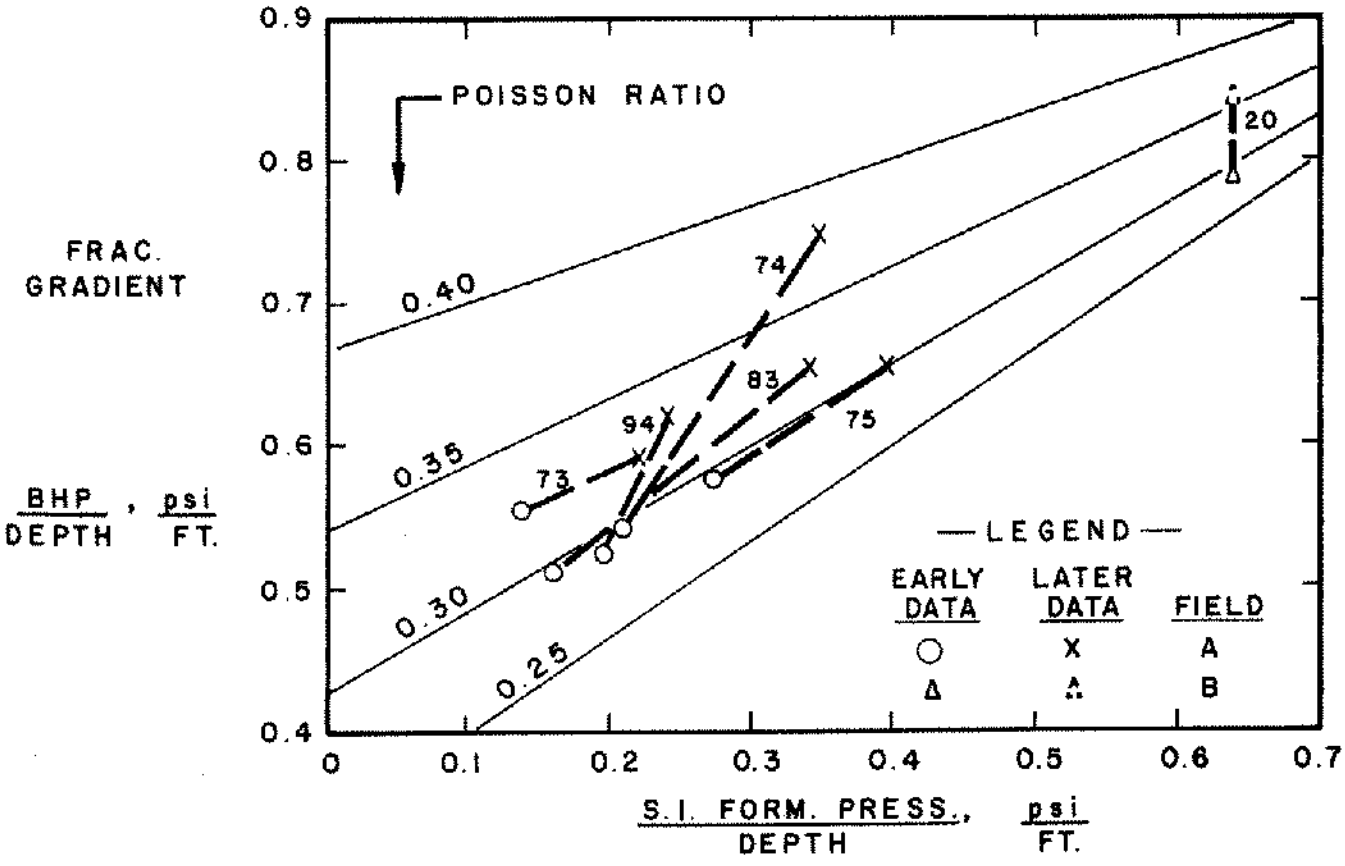

Figure 20. Analysis of fracturing gradients observed during different stages of water injection. Numbers on curves refer to well numbers.

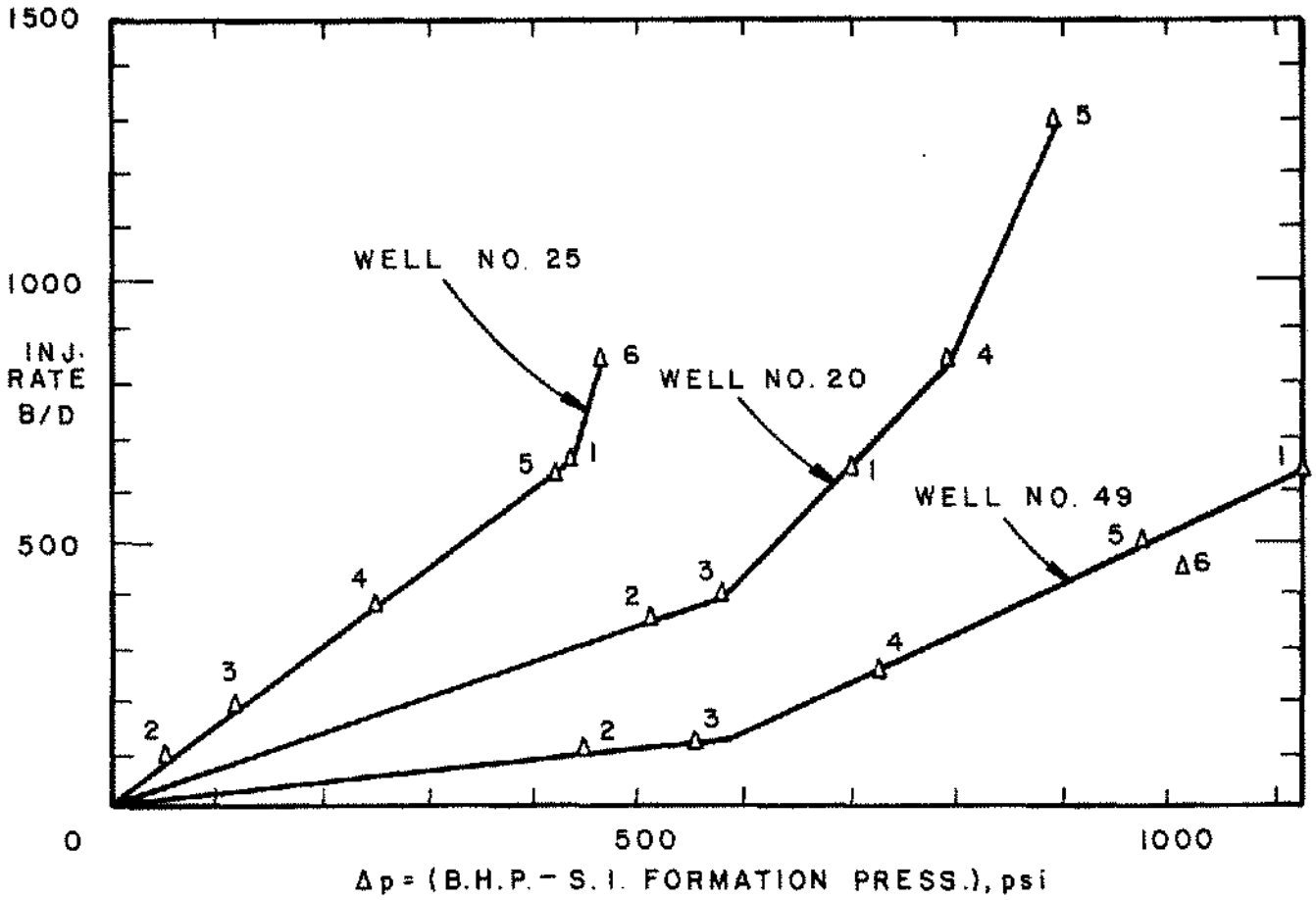

Figure 21. Breaks in step-rate injectivity curves, indicating formation fracturing. Numbers on data points refer to successive times.

1. Overburden stress gradient vs. depth. Such data can be derived from bulk densities taken from logs, seismic data or shale density measurements. A plot of bulk density vs. depth can then be converted to a plot of average overburden stress gradient vs. depth. (See Figs. 11–12 for such data developed.)

2. Actual fracture pressure gradients for several depths. These can be lost-circulation or squeeze data or actual fracturing data.

3. Formation pressures that apply to the data in Item 2. (In Items 2 and 3, the depths must correspond.)

With these data and Equation 15, the Poisson's ratio curve for the area can be back-calculated and plotted vs. depth. The result will be a curve similar to those of Figure 8. With these curves and Figure 14, fracture gradients can be predicted quite easily and quickly. These values can be plotted as a function of depth and the resulting curves can be used in all the operations previously described.

FRACTURE ORIENTATION

The orientation of the planes of hydraulically induced fractures has been the subject of many heated discussions. One should read the discussion at the end of the paper by Hubbert and Willis and the author's reply to the discussion to fully appreciate the nature of the controversy.

If one examines the complete development of Equation 14, it will become clear that horizontal fractures are not likely to be produced by applied wellbore pressure. It has been shown repeatedly that the planes of the induced fractures are perpendicular to the least principle stress. Figure 1 shows a rock element subjected to the three principle stresses. Since in most cases the entire stress state is caused by the overburden load, σ_z is usually greater than σ_x or σ_y. However, if a formation is subjected or pressures and temperatures that produce plastic failure, then the Poisson's ratio can become as great as 0.5. Also, in some cases, the pore pressure approaches the overburden pressure in magnitude. If either of these situations exist in a formation, the horizontal stress could be equal to the vertical stress. Let's examine equation 14 under each of these conditions. First assume that $\nu = 0.50$

$$\frac{P_w}{D} = \left(\frac{1}{1}\right)\left(\frac{S}{D} - \frac{P_f}{D}\right) + \frac{P}{D}$$

$$\frac{p_w}{D} = \frac{S}{D}$$

Now from equation 3.6

$$\sigma_h = \left(\frac{1}{1}\right) \sigma_z$$

$$\sigma_h = \sigma_z$$

Next, assume that $\frac{p}{D}$ equals $\frac{S}{D}$. Using equation 14, we find that

$$\frac{P_w}{D} = \left(\frac{\nu}{1-\nu}\right)\left(\frac{S}{D} - \frac{S}{D}\right) + \frac{S}{D}$$

or

$$\frac{p_w}{D} = \frac{S}{D}$$

So, in either case, it is very difficult to guess which is the least principal stress. However, these two cases are very rare and the normal situation is that σ_z is much greater than σ_h. Hence, it is the normal situation that the planes of fractures are perpendicular to the direction of the least principal stress and are vertical or nearly so. Fractures propogate away from a wellbore in two directions 180° apart. This behavior has been photographed with borehole cameras and recorded with impression packers. There is little room for doubt that vertical fractures are normally created.

The azimuth of vertical fracture planes is of considerable interest in all oilfield operations. In a given area, it has been found that fracture planes have a preferred orientation with respect to North. Such is presumed to be the case for any localized area and most engineers involved in production and secondary recovery operations appreciate the effect of the fracture pattern on production and injection rates, sweep efficiencies, and profitability. A large volume of literature exists on this aspect of fracture orientation, and it is suggested for further study.[11]

Nomenclature

Symbol	*Definition*	*Units*
D_f	Equivalent depth of lowermost normally pressured formation	ft
K_i	Matrix stress coefficient	—
P	Wellbore pressure	psi
P	Formation pressure	psi
S	Overburden load	psi
Z	Depth	ft
σ	Net effective overburden $\sigma = SZ - P$	psi
ν	Poisson's Ratio	—

REFERENCES

1. Clark, J. B., 1949. A Hydraulic Process for Increasing the Productivity of Oil Wells. *Trans. AIME* 186:1.

2. Howard, G. C. and Scott, P. P., 1951. An Analysis and the Control of Lost Circulation. *Trans. AIME*, 192:171.

3. Hubbert, M. King and Willis, D. G., 1957. Mechanics of Hydraulic Fracturing, *Journal of Petroleum Technology*, (July).

4. Matthews, W. R. and Kelly, John, 1967. How to Predict Formation Pressure and Fracture Gradient. *Oil and Gas Journal*, (February 20).

5. Costley, R. D., 1967. Hazards and Costs Cut by Planned Drilling Programs. *World Oil*, (October):92.

6. Goldsmith, R. and Wilson, G., private communication.

7. Wuerker, R. G., Annotated Tables of Strength and Properties of Rocks, *Petroleum Transactions Reprint Series*, No. 6, Drilling, p. 23.

8. Hottman, C. E. and Johnson, R. K., 1965. Estimation of Formation Pressures from Log-Derived Shale Properties. *Journal of Petroleum Technology*, (June).

9. Eaton, B. A., 1969. Fracture Gradient Prediction and its Application in Oilfield Operations. *Journal of Petroleum Technology*, (October):1353–1360.

10. Filsenthal, Martin and Ferrell, Howard H., 1971. Fracturing Gradients in Waterfloods of Low-Permeability, Partially Depleted Zones. *Journal of Petroleum Technology*, (June):727–730.

11. Pasini, J. III and Overby, W. K., Jr., Natural and Induced Fracture Systems and Their Application in Petroleum Production, *Paper No. SPE 2565*.